

RESEARCH ARTICLE

Flipper stroke rate and venous oxygen levels in free-ranging California sea lions

Michael S. Tift^{1,*}, Luis A. Hückstädt², Birgitte I. McDonald³, Philip H. Thorson⁴ and Paul J. Ponganis¹

ABSTRACT

The depletion rate of the blood oxygen store, development of hypoxemia and dive capacity are dependent on the distribution and rate of blood oxygen delivery to tissues while diving. Although blood oxygen extraction by working muscle would increase the blood oxygen depletion rate in a swimming animal, there is little information on the relationship between muscle workload and blood oxygen depletion during dives. Therefore, we examined flipper stroke rate, a proxy of muscle workload, and posterior vena cava oxygen profiles in four adult female California sea lions (*Zalophus californianus*) during foraging trips at sea. Flipper stroke rate analysis revealed that sea lions minimized muscle metabolism with a stroke–glide strategy when diving, and exhibited prolonged glides during the descent of deeper dives (>100 m). During the descent phase of these deep dives, 55±21% of descent was spent gliding, with the longest glides lasting over 160 s and covering a vertical distance of 340 m. Animals also consistently glided to the surface from 15 to 25 m depth during these deeper dives. Venous hemoglobin saturation (S_{O_2}) profiles were highly variable throughout dives, with values occasionally increasing during shallow dives. The relationship between S_{O_2} and flipper stroke rate was weak during deeper dives, while this relationship was stronger during shallow dives. We conclude that (1) the depletion of oxygen in the posterior vena cava in deep-diving sea lions is not dependent on stroke effort, and (2) stroke–glide patterns during dives contribute to a reduction of muscle metabolic rate.

KEY WORDS: Diving physiology, Flipper stroke rate, Marine mammal, Venous oxygen

INTRODUCTION

Optimal management of oxygen stores underlies the breath-hold capacity of air-breathing divers. The utilization of oxygen stores during dives is dependent on the regulation of heart rate, the magnitude and/or distribution of peripheral blood flow, tissue oxygen uptake and muscle workload. The severe bradycardia and peripheral vasoconstriction observed in the classic dive response conserves oxygen in blood by directing it towards hypoxia-sensitive tissues, such as the brain and heart (Irving et al., 1941; Scholander et al., 1942). However, blood oxygen supplementation to working muscle can occur during moderate bradycardias that are common

during routine dives and breath-holds of diving animals (Guyton et al., 1995; Jobsis et al., 2001; Ponganis et al., 2008; Williams et al., 2011). In addition, the positive relationship between heart rate and flipper stroke rate in some diving mammals has led to the hypothesis that exercise and muscle workload modulate the dive response and increase heart rate during short duration dives (Davis and Williams, 2012). In the presence of muscle blood flow, blood oxygen extraction by working muscles during a dive should result in a decline in venous hemoglobin saturation (S_{O_2}). Such declines in venous oxygen content are proportional to muscle workload in terrestrial mammals, despite increases in muscle blood flow and oxygen delivery during exercise (Taylor et al., 1987).

The California sea lion [*Zalophus californianus* (Lesson 1828)] is an ideal model with which to investigate the effect of muscle workload (flipper stroke rate) on the depletion of blood oxygen stores during dives. These animals are known for being active swimmers and can dive as deep as 540 m and as long as 10 min, during which they demonstrate a wide range of heart rate responses and blood oxygen depletion patterns (Kuhn and Costa, 2014; McDonald and Ponganis, 2012, 2013, 2014). For this study, we equipped free-ranging adult female California sea lions with bio-logging devices that simultaneously recorded depth, tri-axial acceleration and venous partial pressure of oxygen (P_{O_2}). From these data, we documented stroke rate profiles, evaluated the effect of muscle workload on changes in S_{O_2} and determined whether blood oxygen extraction by muscle contributed significantly to S_{O_2} depletion in dives of different depths and durations.

MATERIALS AND METHODS

Instrumentation

This study was conducted on San Nicolas Island, California, in August 2013. Four animals were captured with hoop nets, transferred approximately 1000 m from the capture location site and anesthetized using a portable vaporizer-breathing circuit set up with an initial mixture of 5% isoflurane and 100% oxygen. Once anesthetized, a custom-built P_{O_2} datalogger (UUB-2PT; UFI, Morro Bay, CA, USA) with custom housing (Meer Instruments, Palomar Mountain, CA, USA), time-depth recorder with three-axis accelerometer (TDR10±2 g; Wildlife Computers, Redmond, WA, USA) and VHF radio transmitter (mm160B; Advanced Telemetry Systems, Isanti, MN, USA) were affixed to the dorsal, midline pelage of the animal using epoxy (Loctite, Henkel Corp., Westlake, OH, USA). Using an ultrasound machine (SonoSite Inc., Bothell, WA, USA), the caudal gluteal vein was identified and percutaneously catheterized with a peel-away catheter (5 Fr, Cook Medical, Bloomington, IN, USA). A P_{O_2} electrode (Licox C1.1, Integra Life Sciences, Plainsboro, NJ, USA) was then inserted in the catheter and threaded up into the posterior vena cava. To prevent water damage to the P_{O_2} electrode while out at sea, the P_{O_2} electrode was connected to a waterproof cable and connector (Impulse Enterprise, San Diego, CA, USA). To protect and secure the

¹Scripps Institution of Oceanography, University of California San Diego, Center for Marine Biodiversity and Biomedicine, 8655 Kennel Way, La Jolla, CA 92037, USA.

²Department of Ecology and Evolutionary Biology, University of California Santa Cruz, Long Marine Lab, 100 Shaffer Road, Santa Cruz, CA 95060, USA. ³Moss Landing Marine Laboratories, 8272 Moss Landing Road, Moss Landing, CA 95039, USA. ⁴Institute of Marine Sciences, University of California Santa Cruz, Long Marine Laboratory, 100 Shaffer Road, CA 95060, USA.

*Author for correspondence (tift.mike@gmail.com)

© M.S.T., 0000-0002-0563-0509

electrode, the insertion site was covered with a small patch of neoprene that was affixed to the animal's fur with fast-setting glue (Loctite 401, Henkel). These procedures and calibrations have been explained in more detail in previous publications (McDonald and Ponganis, 2013; Meir et al., 2009; Ponganis et al., 1991, Ponganis et al., 1997, 2007; Stockard et al., 2007). Depth and P_{O_2} were recorded at 1 Hz, and three axes of acceleration were recorded at 16 Hz.

After instrumentation, the animals were placed in a large canine kennel to allow them to safely recover from anesthesia (~30–60 min) and weighed (± 0.2 kg, MSI-7200 Dyna-link; Measurement Systems International, Seattle, WA, USA). Once the animals were fully alert, they were released back onto the same beach from which they were originally captured. We recaptured the sea lions after one to three trips to sea, removed the instruments under manual restraint, and released them (~5–10 min procedure). All procedures were approved by the University of California, San Diego, Animal

Subjects Committee (no. S11303) and National Marine Fisheries Services (no. 14676).

Data processing and statistics

Dive data were analyzed using a custom-written MATLAB program (MathWorks, IKNOS; Y. Tremblay). Briefly, this dive analysis program calculates a zero-offset correction at the surface and identifies dives using a specified minimum depth (10 m) and duration (20 s). This depth threshold was selected as dives under 10 m were too short to evaluate changes in physiological parameters. The following dive phases were identified in the data: descent (surface to 80% maximum depth), bottom (depths within 80% maximum depth) and ascent (80% maximum depth to surface). Most California sea lion dives are shallower than 100 m, yet many adult female California sea lions from San Nicolas Island are known to be deep divers (Kuhn and Costa, 2014; McHuron et al., 2016). Therefore, to compare shallow and deep dives, dives to

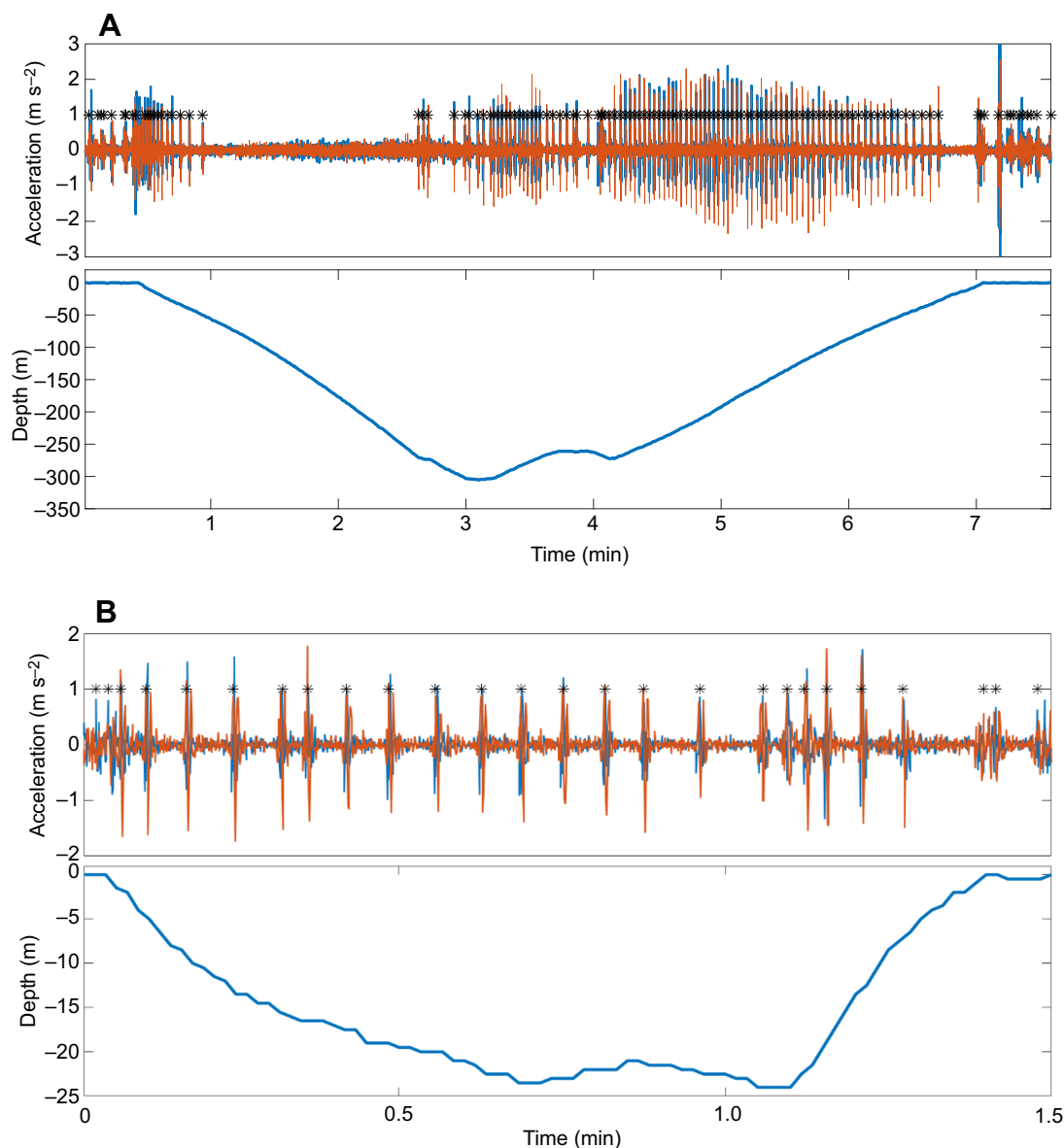


Fig. 1. Identified flipper strokes for a deep and shallow dive from a free-ranging adult female California sea lion. Flipper stroke detection in (A) deep (>100 m) and (B) shallow (≤ 100 m) dive using two axes of acceleration [x (blue)=surge, and z (orange)=heave]. Identified strokes are noted with asterisks. During the deep dive, gliding periods occur during the descent and ascent portions of the dive.

Table 1. Dive characteristics from four adult female California sea lions

Sea lion ID	Mass (kg)	Standard length (m)	No. dives	Mean dive duration (s)	Mean dive depth (m)	No. of deep dives (>100 m)	No. of shallow dives (\leq 100 m)
21314	91.8	1.74	1046	181.7 \pm 141.2 (13–504)	127.2 \pm 128.2 (10–424)	393	653
21316	85.8	1.75	514	119.9 \pm 76.6 (17–470)	57.5 \pm 102.5 (10–385)	76	438
210034	93.2	1.70	1294	132.6 \pm 86.1 (15–376)	77.5 \pm 71.6 (10–289.5)	369	925
210036	71.6	1.60	433	165.7 \pm 68.0 (15–466)	97.5 \pm 53.8 (10–377.5)	265	168
Summary			3287	150.4 \pm 106.6 (13–504)	92.6 \pm 94.9 (10–424)	1103	2184

Values for dive duration and dive depth represent means \pm s.d., while values in parentheses represent the range of values collected.

maximum depths >100 m were classified as deep, and dives to maximum depths \leq 100 m were classified as shallow.

Foreflipper stroke rate was calculated using a custom-written algorithm in MATLAB. The low-frequency static acceleration data were filtered out using a 0.2 Hz high-pass Butterworth filter.

The resulting dynamic acceleration was then analyzed using power spectral density analysis to identify the dominant frequency of a stroke for each individual animal (approximately 0.8–1.2 strokes s^{-1}). A peak detection algorithm, similar to those in other studies (Jeanniard-du-Dot et al., 2016; Sato et al., 2011), was

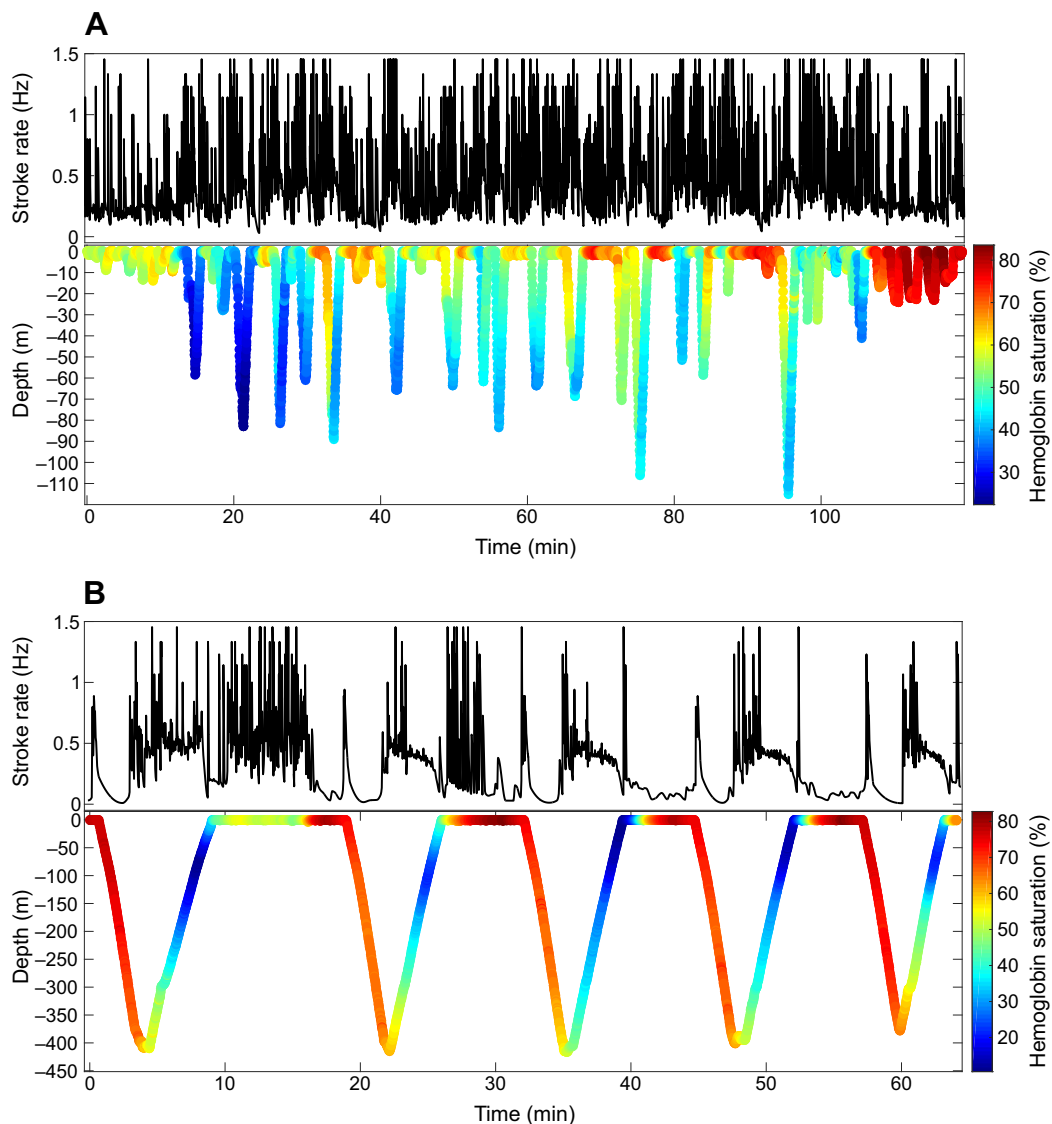


Fig. 2. Hemoglobin saturation and flipper stroke rate for a series of shallow and deep dives from a free-ranging California sea lion. Flipper stroke rate and depth profiles color-coded with posterior vena caval hemoglobin saturation (S_{O_2}) for (A) shallow (\leq 100 m) and (B) deep (>100 m) dives. Note the wide variations in both flipper stroke rates and S_{O_2} during shallow dives, while deep dives exhibit repetitive cyclic patterns.

used to identify flipper strokes. A single flipper stroke was identified when there was a prominent acceleration peak ($\geq 0.4\text{--}0.5\text{ m s}^{-2}$) in the x -axis ('forward surge') or z -axis ('heave surge') (Fig. 1). Stroke rate was calculated as an average stroke rate along a moving window of 10 s throughout the diving record.

The P_{O_2} electrodes were calibrated in the laboratory before deployment (Ponganis et al., 2007; Stockard et al., 2007). Values of S_{O_2} were calculated using the hemoglobin–dissociation curve from McDonald and Ponganis (2013). Because the minimum calculated aerobic dive limit for this species is 3.4 min (Weise and Costa, 2007) and increased P_{CO_2} contributes to a decrease in pH as dive duration increases (Kooyman et al., 1980), P_{O_2} values collected prior to 3 min into the dive were converted to S_{O_2} using the equation for a pH of 7.4 ($\log[S_{O_2}/(100-S_{O_2})]=2.473\times\log(P_{O_2})-3.632$) and all P_{O_2} values collected beyond 3 min into the dive were converted to S_{O_2} using the equation for a pH of 7.3 ($\log[S_{O_2}/(100-S_{O_2})]=2.363\times\log(P_{O_2})-3.576$). Previous data suggest that California sea lions, and other deep-diving pinnipeds, typically keep core body temperature relatively constant at 37°C while diving (McDonald and Ponganis, 2013; Meir and Ponganis, 2010); therefore, P_{O_2} electrodes were only calibrated at this temperature and temperature effects on the S_{O_2} values were not considered. The time on the TDR/accelerometer instrument and P_{O_2} logger were synchronized to the same internet-synced computer clock. Mean change in S_{O_2} (ΔS_{O_2} , $\Delta\% \text{ s}^{-1}$) was calculated for the same 10-s moving window as flipper stroke rates to facilitate comparison. The mean ΔS_{O_2} was also calculated for the three dive phases (descent, bottom and ascent) and the total dive duration.

To investigate whether flipper stroke rate activity affects ΔS_{O_2} for dives of different durations, we used linear mixed-effect models with flipper stroke rate, dive duration and an interaction term (flipper stroke rate \times dive duration) as fixed effects and individual as a random effect. This model was evaluated independently for shallow and deep dives.

Gliding (i.e. no flipper strokes recorded) was consistently noticed during the descent and ascent phases of dives deeper than 100 m. While dives shallower than 100 m did periodically include periods of gliding, the glides were often too short in duration to examine any impacts on diving physiology. The starting and ending depths of the glide and glide durations were independently compared against mass, maximum depth and ΔS_{O_2} for those phases of the dives using a linear mixed-effect model, with individual as the random effect. All linear mixed-effect models were evaluated in JMP (V.12, SAS Institute, Cary, NC, USA) using a built-in LME function and random slope or random intercept model. Corrected Akaike's information criterion (AIC_c) values between these two models were then evaluated; however, the random intercept model always gave the lowest AIC_c value and therefore this model was consistently used. Residuals were visually assessed for normal distribution to determine the quality of the model predictions.

RESULTS

Venous P_{O_2} , depth and acceleration data were simultaneously collected from four adult female California sea lions. This resulted in data collection from a total of 3287 dives. Flipper stroke rate analysis revealed a stroke–glide pattern with periods of prolonged gliding during the descent of deep dives (Fig. 1A). Gliding occasionally occurred in dives shallower than 100 m; however, the glides were brief and inconsistent between these shallower dives. Similar to previous reports on California sea lions from San Nicolas Island (McDonald and Ponganis, 2013, 2014; McHuron et al., 2016), all animals reached depths over 200 m, while the majority

(52%) of dives were shallower than 50 m. The distribution of maximum dive depths was bimodal, with very few dives (11%) occurring at depths of 100–150 m. This bimodal pattern influenced how we defined shallow (≤ 100 m) and deep (>100 m) dives. Dive statistics are reported in Table 1.

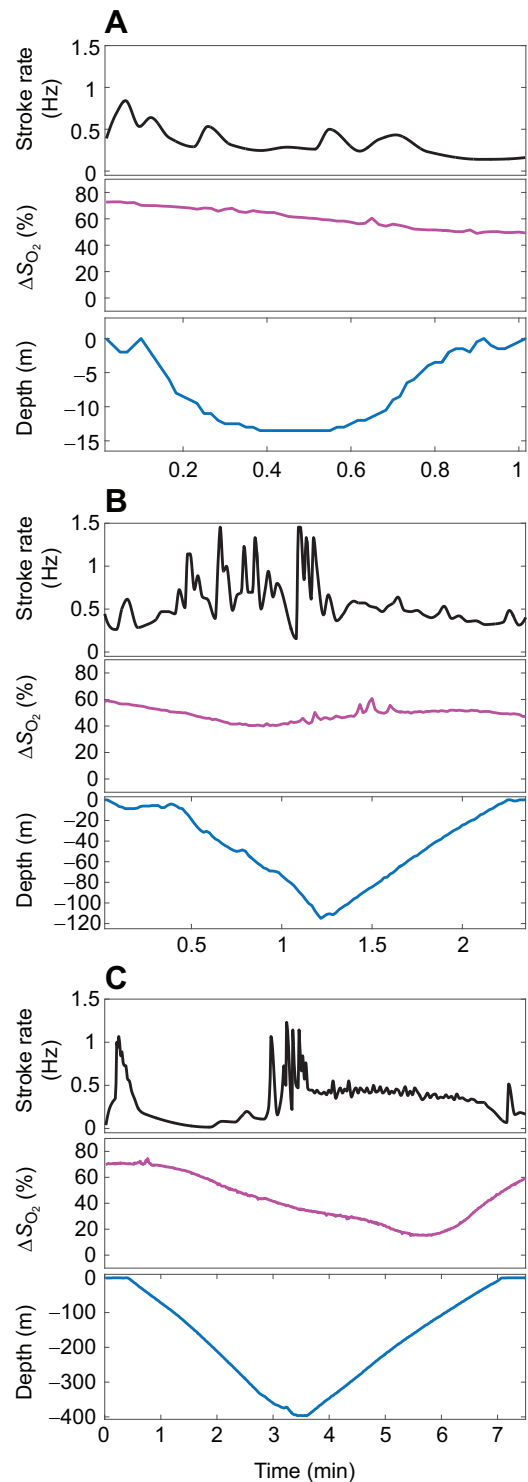


Fig. 3. Comparison of flipper stroke rate and change in hemoglobin saturation for three different dive depths from an adult female free-ranging California sea lion. Flipper stroke rate (black), posterior vena caval hemoglobin saturation (pink) and dive depth profiles (blue) during dives to three different depths [(A) 13 m, (B) 117 m and (C) 395 m].

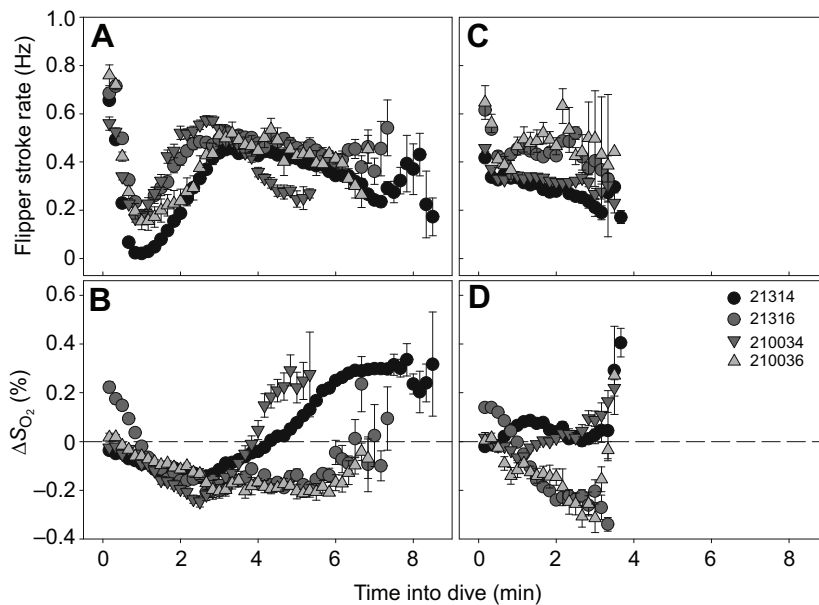


Fig. 4. Mean values for flipper stroke rate and change in hemoglobin saturation during shallow and deep dives. Mean \pm s.e.m. values of flipper stroke rate (A,B) and ΔS_{O_2} (C,D) every 10 s into dives. A and C represent deep dives (>100 m), while B and D represent shallow dives (\leq 100 m). Data are represented for the four individual sea lions from the study. Negative values of ΔS_{O_2} denote oxygen depletion and positive values denote a gain of oxygen for that given 10 s period.

Posterior vena caval S_{O_2} profiles were variable during shallow dives, with a wide range of values throughout dives and inconsistent patterns in ΔS_{O_2} (Fig. 2A). On deeper dives, there was a steady drop in S_{O_2} throughout the dive until later in ascent, when values often increased prior to surfacing (Figs 2B, 3C, 4C). There was no significant relationship between flipper stroke rate and ΔS_{O_2} during deep dives (Table 2). However, there was a significant relationship between the interaction term of dive duration and flipper stroke rate with ΔS_{O_2} during shallow dives (Table 2).

On deeper dives, animals would regularly glide down to depth (Figs 1A, 2B, 3C). This resulted in low stroke rates during the descent of deep dives (Fig. 5). The depth at which gliding started (mean = 60.5 ± 1.6 m; Table 3) on the descent phase of deeper dives did not vary with maximum depth of the dives ($P=0.8$; Table 3). During deep dives, sea lions glided an average of 55% of both the depth and duration of the descent phase, with a maximum of 88% of the descent depth and 92% of the descent duration. As expected, the duration of the descent glide increased significantly with maximum depth of the dive ($F_{1,159}=59.3$, $P<0.001$). The depth at which the descent glide started did not significantly predict patterns of ΔS_{O_2} during the descent period ($P=0.8$).

The average flipper stroke rate was 0.42 ± 0.002 Hz during the ascent phase of deeper dives (Fig. 5). However, ascent flipper stroke rates usually were higher at the beginning of the ascent (~ 1 Hz) and tapered off to a glide by the time the animals reached 15–25 m (Figs 1A, 3C). The depth at which the glide started varied between individuals, and this was not influenced by sea lion mass or dive

depth or duration. At the end of the ascent from deeper dives, animals would also utilize a gliding strategy to reach the surface (Figs 1A, 3C). The depth at which gliding started on the ascent phase did not vary with maximum depth of the dive ($P=0.6$). The duration of the ascent glide did not vary significantly with maximum depth ($P=0.5$). The depth at which gliding started on the ascent phase and the duration of the ascent glide phase were not related to ΔS_{O_2} during the ascent phase ($P=0.3$, $P=0.2$, respectively) (Table 3).

In contrast to the consistent stroke rate patterns seen in deep dives (Figs 2B, 5), our data showed that there was a large variation in flipper stroke rates on dives with maximum depths shallower than 100 m (Figs 2A, 5). Similar to deep dives, the highest stroke rates during shallow dives occurred at the beginning of the dive, while the lowest stroke rates were often at the end of the dive (Figs 3A, 4B). This pattern is consistent with expected buoyancy changes with depth. Overall, the mean flipper stroke rate for the entire dive duration was similar between both shallow dives and deep dives (Fig. 5). However, the range and variability of flipper stroke rates for the entire dive duration was larger during shallow dives (Fig. 5).

DISCUSSION

Flipper stroke patterns

We documented flipper stroke rate patterns in free-ranging adult female California sea lions for the first time. Similar to techniques using one axis of acceleration to identify flipper strokes in free-diving animals (Maresh et al., 2014; Sato et al., 2003), we used both the surge (x) and heave (z) acceleration axes to reliably identify

Table 2. Results from a linear mixed-effect model with dive duration, flipper stroke rate and the interaction between dive duration and flipper stroke rate as fixed effects against ΔS_{O_2}

Depth phase	Fixed effects	Mean ΔS_{O_2}	s.e.m.	d.f.	t	P
Shallow	Intercept	-0.6843	0.324	9659	-2.1	0.0349
	Dive duration (min)	-0.0002	0.001	9659	-0.1	0.8839
	Stroke rate (Hz)	1.9518	0.290	9659	6.7	<0.001
	Dive duration \times Stroke rate	-0.0065	0.003	9659	-2.6	0.0094
Deep	Intercept	-0.6183	0.296	12468	-2.1	0.0370
	Dive duration (min)	-0.0008	0.001	12468	-1.7	0.0891
	Stroke rate (Hz)	0.4321	0.366	12468	1.2	0.2372
	Dive duration \times Stroke rate	-0.0010	0.001	12468	-1.0	0.3360

Individual was the random effect. Values of flipper stroke rate and ΔS_{O_2} were averaged every 10 s into the dive record.

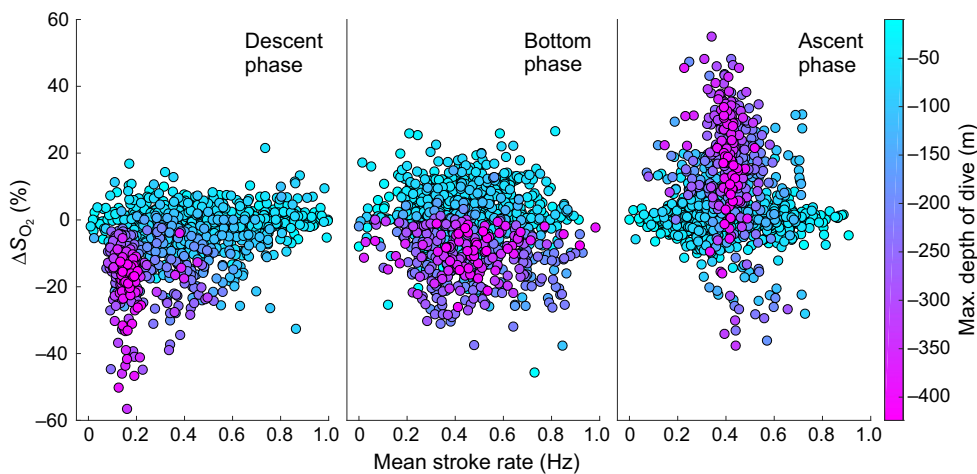


Fig. 5. Mean flipper stroke rate and mean ΔS_{O_2} for the three different dive phases. Each point represents the mean value for a given phase during one dive. Points are color-coded based on the maximum depth of that individual dive. Negative values of ΔS_{O_2} denote oxygen depletion and positive values denote a gain of oxygen.

flipper strokes in all dive phases (Fig. 1). Our results show that the average flipper stroke rates during different dive phases from this study were consistent with data from other free-ranging otariids (~0.4–0.6 Hz; Fig. 5) (Insley et al., 2008; Jeanniard-du-Dot et al., 2016). Similar to some free-ranging phocids and cetaceans (Davis et al., 2001; Williams et al., 2000), California sea lions exhibited periods of gliding on the descent and ascent phases of deep dives, with maximum glides reaching over 160 s and covering 340 m vertical distance on the descent portions (Figs 1A, 2B, 3C). California sea lions are streamlined, with high fineness ratios resulting in low drag, making them efficient at gliding through the water (Feldkamp, 1987). Gliding during descent will conserve blood and muscle oxygen stores for subsequent activities such as prey capture and stroke effort during ascent.

Prolonged gliding on the descent phase was consistently associated with dives that reached the range of the estimated depth of lung collapse in this species (~200 m; Fig. 5) (McDonald and Ponganis, 2012). The average depth at which gliding started on the descent was relatively shallow at around 60 m, yet this is not surprising as buoyancy will decrease as lung volume decreases (approximately 50% of surface lung volume at 10 m depth, and 14% at 60 m according to Boyle's law). Interestingly, elephant seals also began prolonged glides during deep dives at approximately 60 m depth (Davis et al., 2001). The gliding pattern seen on the ascent phase of sea lions has also been documented in other marine mammals and diving birds, and was suggested to be influenced by respiratory air volume (Sato et al., 2011; Watanuki et al., 2006; Williams et al., 2000). Ascent glides in sea lions are likely secondary to increased buoyancy near the surface owing to lung re-expansion during ascent.

Relationship of blood oxygen use to flipper stroke rate in shallow dives

Profiles of S_{O_2} were highly variable during shallow dives, with S_{O_2} even increasing throughout the duration of the dive (Figs 2A,

4D). In addition, some shallow dives began with low S_{O_2} ; the sea lions did not completely re-saturate venous blood prior to starting these dives (Fig. 2A). In some cases, ΔS_{O_2} appeared to be affected by stroke rate patterns as would be expected during exercise and consistent with recent suggestions that heart rate (and presumably some muscle blood flow) is modulated by exercise (Davis and Williams, 2012; Williams et al., 2015). During shallow dives, California sea lions exhibit higher heart rates than those seen during deep dives (McDonald and Ponganis, 2014). These higher heart rates are likely associated with increased blood flow to muscle, and could account for the relationship between flipper stroke rates and venous blood oxygen depletion during shallow dives. However, the weak correlation between the two parameters, and in some instances, increases in S_{O_2} throughout the dives, despite high stroke rates, argues that this does not always occur.

Full interpretation of S_{O_2} during shallow dives is also limited by the lack of arterial hemoglobin saturation data during shallow dives of California sea lions. The relationship between S_{O_2} profiles and the interaction of dive duration and stroke rate of shallow dives may also be partially secondary to increased heart rates, muscle perfusion and greater arterial hemoglobin desaturation during longer shallow dives. In other words, a decrease in S_{O_2} may reflect a decrease in arterial oxygen content delivery rather than an increase in blood oxygen extraction by tissue. Ideally, simultaneous measurements of arterial/venous blood oxygen content, heart rate, flipper stroke patterns and/or muscle myoglobin saturation would resolve this question.

From our current data, it appears that for shallow, short duration dives, regulation of posterior vena caval S_{O_2} is not critical or highly controlled, and that the peripheral vascular response is quite variable. Such plasticity in blood flow distribution has also been observed in diving emperor penguins (Williams et al., 2011).

Table 3. Total glide durations and depths of the start and end of the descent and ascent gliding periods for four California sea lions on dives deeper than 100 m ($n=175$ dives)

Animal ID	Descent glide start (m)	Descent glide end (m)	Descent glide duration (s)	Ascent glide start (m)	Ascent glide end (m)	Ascent glide duration (s)
21314	46.6±1.8	234.0±10.8	89.5±4.7	24.3±0.5	6.0±0.4	11.0±0.4
21316	77.0±2.6	221.7±10.8	75.5±6.0	15.2±0.7	1.2±0.7	7.5±0.3
210034	60.3±3.3	134.2±6.0	35.9±3.4	20.6±0.5	3.7±0.3	9.5±0.3
210036	61.4±3.6	199.4±10.6	76.7±6.1	19.8±0.9	1.7±0.2	10.3±0.5
Total mean (range)	60.5±1.6 (13.5–147)	199.8±5.8 (55–388)	70.5±3.0 (6.5–161.0)	20.3±0.4 (4.5–33)	3.4±0.2 (0–12.5)	9.6±0.2 (2.8–16.2)

The total mean values are reported ±s.e.m.

Relationship of blood oxygen use to flipper stroke rate in deep dives

Assessment of locomotory effort on S_{O_2} profiles during deep dives is aided by our prior study that demonstrated that arterial hemoglobin saturation is maintained during dives over 300 m deep and 6 min in duration (McDonald and Ponganis, 2012). Consequently, changes in S_{O_2} during deep dives are more likely because of changes in perfusion and tissue oxygen extraction rather than a decrease in arterial oxygen content delivery.

Posterior vena caval S_{O_2} profiles in the sea lions were similar to those of a previous study from our laboratory (McDonald and Ponganis, 2013). In the present study, we demonstrate that flipper stroke rates had little impact on ΔS_{O_2} during a majority of deep dives of sea lions (Table 2). We also saw that S_{O_2} often increased during the ascent, despite the animal's active stroking to reach the surface (Figs 2B, 3C, 4C). Furthermore, the greatest decreases in S_{O_2} occurred during the low stroke rates and prolonged glides of the descents of deep dives (Figs 3, 5). In contrast, some of the largest increases in S_{O_2} occurred while the animals were actively stroking during ascent from deep dives (Figs 3C, 5). As in our prior studies, we postulate that the re-oxygenation of venous blood prior to surfacing is indicative of maintenance of pulmonary gas exchange at shallow depths, increased peripheral perfusion and possible use of arterio-venous shunts during the ascent (McDonald and Ponganis, 2012, 2013, 2014).

Based on these findings, we conclude that ΔS_{O_2} in the posterior vena cava is not significantly affected by flipper stroke rate during deep dives. Rather, as we have previously hypothesized (McDonald and Ponganis, 2013), it is more likely that S_{O_2} is determined by the degree of bradycardia, the magnitude of reduction in peripheral blood flow and the associated changes in tissue transit time during dives. Prolonged tissue transit times during severe bradycardia should result in greater blood oxygen extraction and lower hemoglobin saturations in any blood slowly draining into the posterior vena cava. In addition, given that arterial hemoglobin saturation is well maintained throughout deep dives (McDonald and Ponganis, 2012), desaturation of venous blood is unlikely secondary to a decrease in arterial blood oxygen content.

The maintenance of high arterial hemoglobin saturation (McDonald and Ponganis, 2012), despite the posterior vena caval S_{O_2} decreasing to extremely low values during deep dives, suggests the presence of a central venous oxygen pool that is slowly depleted during the severe bradycardias seen in deep dive (McDonald and Ponganis, 2014). Otherwise, in the presence of lung collapse and lack of gas exchange, arterial hemoglobin saturation should reflect the low venous values observed in the posterior vena cava. Such a central blood oxygen store would be analogous to the hepatic sinus oxygen store described in elephant seals (Elsner et al., 1964). The existence of such a central venous oxygen store remains to be demonstrated in otariids with either anterior vena cava or pulmonary artery hemoglobin saturation measurements.

Conclusions

California sea lions use a gliding strategy during the descent phase of most dives beyond 100 m. On these deeper dives, animals also glide to the surface from depths of 15–25 m, probably because of the increased buoyancy associated with lung re-expansion during ascent. The lack of a strong relationship between posterior vena caval S_{O_2} and flipper stroke rate during deep and some shallow dives demonstrates that posterior vena caval hemoglobin desaturation is not dependent on muscle work load. This independence of blood oxygen depletion from locomotory effort implies that (1) muscle

blood flow is restricted during deep dives, and not consistently regulated during shallow dives, and (2) the posterior vena caval oxygen profile is more related to heart rate and the magnitude of tissue perfusion and/or oxygen extraction.

Acknowledgements

The logistics and field work for this project were made possible by the intense efforts from many volunteers, and we are very thankful for their help. Specifically, we would like to thank J. Ugoretz, G. Smith, G. Kooyman, R. Walsh, E. McHuron, C. Verlinden, C. Stehman, D. Costa and many other members of the Costa lab at UCSC.

Competing interests

The authors declare no competing or financial interests.

Author contributions

P.J.P. obtained the grant. M.S.T., P.J.P. and B.I.M. conceived the experiments. M.S.T., P.J.P., L.A.H. and P.H.T. collected the data. M.S.T. and L.A.H. performed the analyses. M.S.T. and P.J.P. wrote the manuscript. B.I.M. and L.A.H. edited the manuscript.

Funding

This work was supported by Office of Naval Research grant N000141410404.

References

- Davis, R. W. and Williams, T. M. (2012). The marine mammal dive response is exercise modulated to maximize aerobic dive duration. *J. Comp. Physiol. A* **198**, 583–591.
- Davis, R. W., Fuiman, L. A., Williams, T. M. and Le Boeuf, B. J. (2001). Three-dimensional movements and swimming activity of a northern elephant seal. *Comp. Biochem. Physiol. A Mol. Integr. Physiol.* **129**, 759–770.
- Elsner, R. W., Scholander, P. F., Craig, A. B., Dimond, E. G., Irving, L., Pilson, M., Johansen, K. and Bradstreet, E. (1964). A venous blood oxygen reservoir in the diving elephant seal. *Physiologist* **7**, 124.
- Feldkamp, S. D. (1987). Swimming in the California sea lion: morphometrics, drag and energetics. *J. Exp. Biol.* **131**, 117–135.
- Guyton, G. P., Stanek, K. S., Schneider, R. C., Hochachka, P. W., Hurford, W. E., Zapol, D. G., Liggins, G. C. and Zapol, W. M. (1995). Myoglobin saturation in free-diving Weddell seals. *J. Appl. Physiol.* **79**, 1148–1155.
- Insley, S. J., Robson, B. W., Yack, T., Ream, R. R. and Burgess, W. C. (2008). Acoustic determination of activity and flipper stroke rate in foraging northern fur seal females. *Endangered Species Res.* **4**, 147–155.
- Irving, L., Scholander, P. F. and Grinnell, S. W. (1941). Significance of the heart rate to the diving ability of seals. *J. Cell. Physiol.* **18**, 283–297.
- Jeanniard-du-Dot, T., Trites, A. W., Arnould, J. P. Y., Speakman, J. R. and Guinet, C. (2016). Flipper strokes can predict energy expenditure and locomotion costs in free-ranging northern and Antarctic fur seals. *Sci. Rep.* **6**, 33912.
- Jobsis, P. D., Ponganis, P. J. and Kooyman, G. L. (2001). Effects of training on forced submersion responses in harbor seals. *J. Exp. Biol.* **204**, 3877–3885.
- Kooyman, G. L., Wahrenbrock, E. A., Castellini, M. A., Davis, R. W. and Sinnett, E. E. (1980). Aerobic and anaerobic metabolism during voluntary diving in Weddell seals: evidence of preferred pathways from blood chemistry and behavior. *J. Comp. Physiol. B* **138**, 335–346.
- Kuhn, C. E. and Costa, D. P. (2014). Interannual variation in the at-sea behavior of California sea lions (*Zalophus californianus*). *Mar. Mamm. Sci.* **30**, 1297–1319.
- Maresh, J. L., Simmons, S. E., Crocker, D. E., McDonald, B. I., Williams, T. M. and Costa, D. P. (2014). Free-swimming northern elephant seals have low field metabolic rates that are sensitive to an increased cost of transport. *J. Exp. Biol.* **217**, 1485–1495.
- McDonald, B. I. and Ponganis, P. J. (2012). Lung collapse in the diving sea lion: hold the nitrogen and save the oxygen. *Biol. Lett.* **8**, 1047–1049.
- McDonald, B. I. and Ponganis, P. J. (2013). Insights from venous oxygen profiles: oxygen utilization and management in diving California sea lions. *J. Exp. Biol.* **216**, 3332–3341.
- McDonald, B. I. and Ponganis, P. J. (2014). Deep-diving sea lions exhibit extreme bradycardia in long-duration dives. *J. Exp. Biol.* **217**, 1525–1534.
- McHuron, E. A., Robinson, P. W., Simmons, S. E., Kuhn, C. E., Fowler, M. and Costa, D. P. (2016). Foraging strategies of a generalist marine predator inhabiting a dynamic environment. *Oecologia* **182**, 995–1005.
- Meir, J. U. and Ponganis, P. J. (2010). Blood temperature profiles of diving elephant seals. *Physiol. Biochem. Zool.* **83**, 531–540.
- Meir, J. U., Champagne, C. D., Costa, D. P., Williams, C. L. and Ponganis, P. J. (2009). Extreme hypoxemic tolerance and blood oxygen depletion in diving elephant seals. *Am. J. Physiol. Regul. Integr. Comp. Physiol.* **297**, R927–R939.

- Ponganis, P. J., Kooyman, G. L. and Zornow, M. H.** (1991). Cardiac output in swimming California sea lions, *Zalophus californianus*. *Physiol. Zool.* **64**, 1296-1306.
- Ponganis, P. J., Kooyman, G. L., Winter, L. M. and Starke, L. N.** (1997). Heart rate and plasma lactate responses during submerged swimming and trained diving in California sea lions, *Zalophus californianus*. *J. Comp. Physiol. B* **167**, 9-16.
- Ponganis, P. J., Stockard, T. K., Meir, J. U., Williams, C. L., Ponganis, K. V., van Dam, R. P. and Howard, R.** (2007). Returning on empty: extreme blood O₂ depletion underlies dive capacity of emperor penguins. *J. Exp. Biol.* **210**, 4279-4285.
- Ponganis, P. J., Kreutzer, U., Stockard, T. K., Lin, P.-C., Sailasuta, N., Tran, T.-K., Hurd, R. and Jue, T.** (2008). Blood flow and metabolic regulation in seal muscle during apnea. *J. Exp. Biol.* **211**, 3323-3332.
- Sato, K., Mitani, Y., Cameron, M. F., Siniff, D. B. and Naito, Y.** (2003). Factors affecting stroking patterns and body angle in diving Weddell seals under natural conditions. *J. Exp. Biol.* **206**, 1461-1470.
- Sato, K., Shiomi, K., Marshall, G., Kooyman, G. L. and Ponganis, P. J.** (2011). Stroke rates and diving air volumes of emperor penguins: implications for dive performance. *J. Exp. Biol.* **214**, 2854-2863.
- Scholander, P. F., Irving, L. and Grinnell, S. W.** (1942). On the temperature and metabolism of the seal during diving. *J. Cell. Physiol.* **19**, 67-78.
- Stockard, T. K., Levenson, D. H., Berg, L., Fransioli, J. R., Baranov, E. A. and Ponganis, P. J.** (2007). Blood oxygen depletion during rest-associated apneas of northern elephant seals (*Mirounga angustirostris*). *J. Exp. Biol.* **210**, 2607-2617.
- Taylor, R. C., Karas, R. H., Weibel, E. R. and Hoppeler, H.** (1987). Adaptive variation in the mammalian respiratory system in relation to energetic demand: II. Reaching the limits to oxygen flow. *Respir. Physiol.* **69**, 7-26.
- Watanuki, Y., Wanless, S., Harris, M., Lovvorn, J. R., Miyazaki, M., Tanaka, H. and Sato, K.** (2006). Swim speeds and stroke patterns in wing-propelled divers: a comparison among alcids and a penguin. *J. Exp. Biol.* **209**, 1217-1230.
- Weise, M. J. and Costa, D. P.** (2007). Total body oxygen stores and physiological diving capacity of California sea lions as a function of sex and age. *J. Exp. Biol.* **210**, 278-289.
- Williams, T. M., Davis, R. W., Fuiman, L. A., Francis, J., Le Boeuf, B. J., Horning, M., Calambokidis, J. and Croll, D. A.** (2000). Sink or swim: strategies for cost-efficient diving by marine mammals. *Science* **288**, 133-136.
- Williams, C. L., Meir, J. U. and Ponganis, P. J.** (2011). What triggers the aerobic dive limit? Patterns of muscle oxygen depletion during dives of emperor penguins. *J. Exp. Biol.* **214**, 1802-1812.
- Williams, T. M., Fuiman, L. A., Kendall, T., Berry, P., Richter, B., Noren, S. R., Thometz, N., Shattock, M. J., Farrell, E., Stamper, A. M. et al.** (2015). Exercise at depth alters bradycardia and incidence of cardiac anomalies in deep-diving marine mammals. *Nat. Commun.* **6**, 6055.